Journal of Materials Chemistry C

ROYAL SOCIETY OF CHEMISTRY

PAPER

Published on 13 July 2026

Cite this: DOI: 10.1039/d6tc01479h

Sustainable access to perylenedicarboxylic monoimides and diesters enables processable 3,3′-biperylene derivatives with large Stokes shifts

Lorenza Marcotullio, Mauro Sassi, Anita Zucchi, Francesca Pallini, Luca Beverina and Sara Mattiello *

Received 8th May 2026,
Accepted 8th July 2026

DOI: 10.1039/d6tc01479h

rsc.li/materials-c

Dimeric 3,3′-biperylenes derivatives derived from perylene-3,4-dicarboxylic monoimides (PMIs) and perylene-3,4-diesters (PDEs) represent promising yet underexplored alternatives to classical perylene-3,4,9,10-diimides (PDIs) and perylene-3,4,9,10-tetraesters (PTEs). In contrast to these widely used systems, 3,3′-biperylenes derivatives combine high absorption coefficients with intrinsically large Stokes shifts arising from excited-state structural reorganization, while displaying minimal solvatochromism and reduced aggregation. These features are highly advantageous for wavelength-shifting applications, where reabsorption losses and environmental sensitivity limit the performance of conventional chromophores. Their limited adoption has been primarily dictated by the poor accessibility of 3,4-perylenedicarboxylic monoanhydride (**PDCMA**), the key synthetic intermediate. Here, we leverage a scalable and sustainable synthesis of **PDCMA** to establish a practical platform for the preparation of PMIs, PDEs, and their corresponding dimers. The resulting materials outperform PDIs and PTEs in terms of spectral separation, and can be readily incorporated into photopolymerizable resins to yield transparent, luminescent 3D objects while preserving their optical properties at high loadings.

Introduction

Perylene-based chromophores represent one of the most established and versatile classes of organic functional materials, with applications spanning organic electronics, bioimaging, photocatalysis, and photonics.[1–4] Their success arises from a unique combination of high molar extinction coefficients, outstanding photostability, and well-defined electronic structure. Among them, perylenediimides (PDIs) have dominated both fundamental and applied research, largely due to their excellent optical performances and the widespread availability of their precursor, perylenetetracarboxylic dianhydride (**PTCDA**), a large-scale commodity chemical.[5] However, the intrinsic symmetry and structural rigidity of PDIs impose important limitations, including small Stokes shifts, negligible excited-state polarity, and limited capacity to support charge-transfer (CT) states.

In this context, perylenedicarboxylic monoimides (PMIs) offer a complementary and, in several respects, more versatile photophysical platform. The reduced symmetry of PMI-based architectures introduces donor–acceptor character and enables symmetry-breaking charge-transfer (SB-CT) states in the excited state,[6,7] resulting in large Stokes shifts. These features are particularly attractive for applications where suppression of self-absorption and efficient radiative energy transfer *via* waveguiding are required, such as luminescent solar concentrators and scintillators.[8] Despite these advantages, PMI-based materials—and especially their 3,3′-biperylene analogues (**BPDIs**)—remain significantly underexplored compared to PDIs.[9–11] This imbalance does not reflect

Department of Materials Science, University of Milano-Bicocca, via R. Cozzi 55, 20126, Milan, Italy. E-mail: sara.mattiello@unimib.it

Sara Mattiello

Sara Mattiello was born in 1990 in Milan, Italy. She graduated in Materials Science at the University of Milano-Bicocca in 2014, where she obtained her PhD in 2018 working under the supervision of Prof. Luca Beverina. Since 2025 she has been working as a tenure-track professor in Organic and Materials Chemistry. Her research interests span from optical properties of organic materials, to photochemistry, formulation chemistry, and green chemistry applied to organic electronics. In her spare time, she loves painting, practicing yoga, and role-playing games.

intrinsic material limitations, but rather longstanding synthetic challenges.

In this respect, we recently developed a straightforward, scalable, and sustainable two-step synthesis of 3,4-perylenedicarboxylic monoanhydride (**PDCMA**), the essential building block for PMIs and related derivatives, based on aqueous Suzuki–Miyaura coupling followed by solvent-free Scholl cyclization.[12] This approach eliminates chromatographic purification, avoids chlorinated solvents, and enables multigram-scale preparation with dramatically improved green metrics (*E*-factor $\approx$ 240 *vs.* $>$3000 for previous routes).[13–16] Beyond its synthetic convenience, this methodology aligns with key principles of green chemistry, including solvent minimization, energy efficiency, and waste reduction.

The availability of **PDCMA** through this route fundamentally expands the accessible chemical space of perylene derivatives. In particular, it enables modular access to two largely overlooked families of chromophores: perylenedicarboxylic monoimides (PMIs) and perylene-3,4-diesters (PDEs), as well as their corresponding dimeric 3,3′-biperylene-9,9′,10,10′-tetracarboxylic acid (BPTCA) architectures. In fact, the formers are the typical building blocks needed to prepare the latter (Scheme 1). BPTCA derivatives combine several attractive features: (i) large Stokes shifts arising from a twisted chromophore structure; (ii) absorption coefficients in the order of 10^5 M^{-1} cm^{-1}; (iii) high photoluminescence quantum yields independent from the external environment due to steric restriction of rotation;[17,18] and (iv) improved solubility and processability, which mitigate aggregation issues typical of highly planar perylene cores.[9]

In this work, we systematically compared alternative synthetic routes toward PMIs and PDEs in terms of yield, scalability, and sustainability, and demonstrate that **PDCMA**-based strategies provide clear advantages over traditional **PTCDA**-based approaches. Furthermore, we show that the obtained BPTCA derivatives exhibit favourable photophysical properties, including large Stokes shifts, and reduced aggregation, which can be retained even upon incorporation into solid polymer matrices. In particular, we demonstrate the integration of these dyes into commercially available photopolymerizable resins for additive manufacturing, enabling the fabrication of luminescent 3D objects without loss of optical performance.

By combining sustainable synthesis, improved processability, and functional photophysical properties, this work positions PMI- and PDE-based systems as viable and versatile alternatives to classical perylenediimides for next-generation photonic materials.

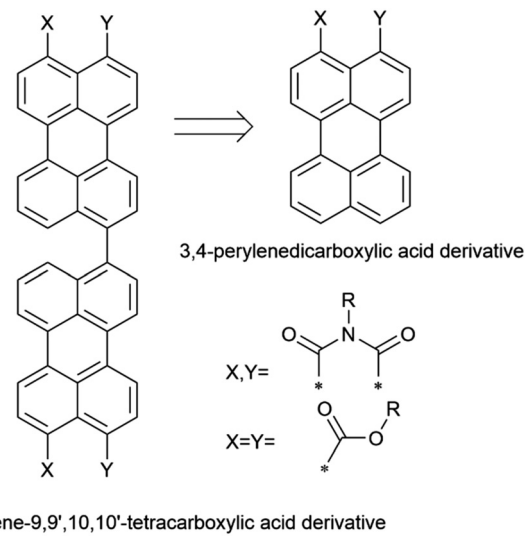

Scheme 1 Retrosynthetic access of 3,3′-biperylene-9,9′,10,10′-tetracarboxylic acid (BPTCA) derivatives.

Results and discussion

Synthetic routes toward BPDIs and BPTEs

Section S4 and S5 of the SI report a complete picture of the literature routes available for the preparation of PMIs, and their assessment in terms of efficiency and sustainability. The most efficient one, requiring only one synthetic step, is the imidation–decarboxylation of **PTCDA** at 190 °C in an autoclave, originally developed by Langhals.[14] We therefore proceeded to prepare three PDIs, bearing different substituents at the nitrogen, both according to this route and by imidation of **PDCMA**, in order to carefully compare the two preparation methods. In particular, we chose one aryl and two alkyl amines among those reported to impart a good solubility to the final product, specifically 2,5-di-*tert*-butylaniline (DTBP), 2-ethylhexylamine (EH), and 9-hexadecylamine (HD). Results are reported in Fig. 1.

Despite requiring three steps instead of one, route B1 remains advantageous over route A for all the three considered imidations: in fact, the PMIs were isolated in 27–54% yield according to route A, while for route B we achieved 60–85% overall yields. The improvement is particularly relevant in the case of alkylamines, as the decarboxylative imidation of **PDCMA** is not as efficient as observed with the aniline, affording **PMI-EH** and **PMI-HD** in 32% and 27% yield respectively. Such numbers align to those reported in the literature for other alkyl monoimides.[14] The yields drop mainly due to the preferential formation of the double imidation products, obtained in 45–55% yield (isolated in 26% yield during the preparation of **PMI-DTBP**). Since in all the cases the amine was used as the limiting reagent, we speculate that this behaviour is due to the higher solubility of the alkylmonoimide monoanhydride, facilitating the second imidation step over the decarboxylation. On the contrary, the imidation of **PDCMA** works smoothly in both cases, affording **PMI-EH** and **PMI-HD** in 98% and 70% yield respectively.

Besides yields, we assessed the synthetic access toward PMIs for the two routes in terms of complete *E*-factor (a green chemistry metrics consisting in the weight ratio of wastes over product).[19]

Purification of PMIs according to route A requires column chromatography to separate the target product from perylene and the corresponding bisimide. This process is very demanding due to the poor solubility of the components and their tendency to saturate the stationary phase, resulting in extensive use of chlorinated solvents and silica. In contrast, route B1 affords

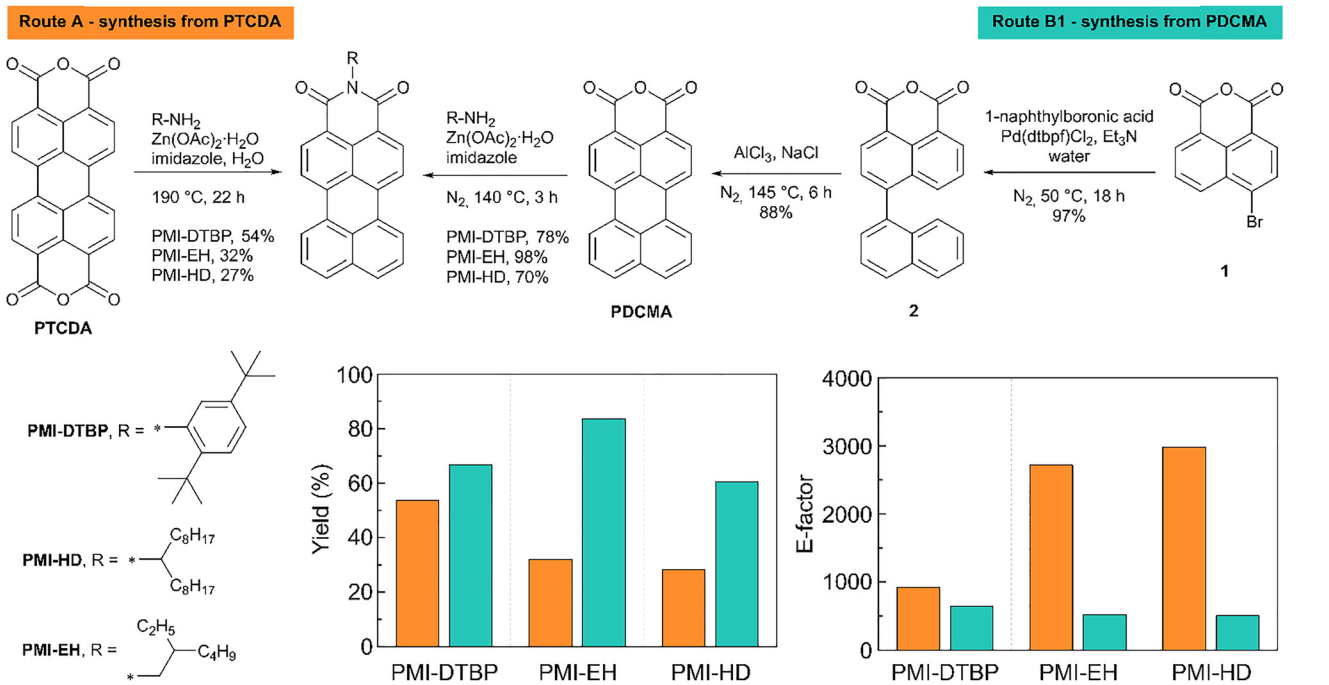

Fig. 1 Synthesis of **PMI-DTBP**, **PMI-EH** and **PMI-HD** according to route A and B1, and associated overall yields (starting from the commercially available precursor **1** for route B1) and *E*-factors for their preparation.

PMIs cleanly in the final step, requiring only a simple filtration on a silica pad to remove insoluble byproducts.

Consequently, the *E*-factors for route B show significant improvement compared to route A, especially for the alkyl-substituted PMIs, where they decrease from nearly 3000 to around 500. The improvement is less marked for **PMI-DTBP**, as we found that 46% of the product can be isolated by crystallization instead of column chromatography, thus lowering the impact of purification.

Taking into account also the time and effort needed to perform the whole syntheses for the different PMIs, we deem to share the following considerations:

- The modest increment in yield and waste reduction obtained for the preparation of **PMI-DTBP** according to route B1 might not compensate for the increased effort needed to perform a three-step procedure with respect to the single reaction needed according to route A.
- The previous consideration likely applies for reactions with different anilines affording a PMI in similar yield and having similar solubility to **PMI-DTBP**.
- On the contrary, it's worth pursuing route B1 when an aliphatic PMI is the target, as products are obtained in substantially higher yields and with a remarkable reduction in the solvents required for purification.
- Whenever a screening for different N-substituents is needed for the development of a product, route B1 is superior, as **PDCMA** can be prepared on quite large scale, and the PMIs purification is easier.

Besides PMIs, **PDCMA** is a very convenient precursor for the preparation of perylene 3,4-diesters (PDEs), which at the moment are nearly absent in the panorama of perylene derivatives due indeed to the difficult synthetic access to **PDCMA**. Two literature protocols for their preparation are reported: the deconstruction route reported by Xiao,[15] and the construction route proposed by Stupp.[16] We evaluated both in terms of efficiency and sustainability (see Section S4.3 of SI), eventually deciding to prepare two PDEs having *n*-butyl and *n*-decyl chains both according to Xiao procedure (with little optimization as explained in SI, Section S3.2), and by esterification of **PDCMA**. Results are shown in Fig. 2.

In both cases, route B2 allows to prepare the target products in higher overall yields (70–80%) with respect to route C (around 53% yield in both cases). Although chromatographic purification is required for both routes in the last step, the crude obtained from **PDCMA** esterification features higher purity than that obtained by decarboxylation of the perylene-monoanhydride diesters **4a–b**, thus the product can be isolated simply by filtration on a silica cake instead of careful column chromatography. This aspect clearly impacts on the overall amount of solvents needed for the synthetic procedures, with *E*-factors that are halved for products isolated according to route B2 with respect to those obtained according to route C.

Having optimized the preparation of both PMI and PDE building blocks, we proceeded with their bromination to obtain the precursors to prepare the target 3,3′-biperylenes.

After careful screening of reaction conditions on **PMI-DTPB** (see SI section 3.3 for details), we chose acetic acid as the solvent and bromine as the electrophile (Scheme 2). Using such conditions, we were able to selectively brominate both **PMI-DTBP** and **PMI-EH** at the 9-position, obtaining both products **5a** and **5b** in 98% yield. Unexpectedly, we found that **PMI-HD** does not behave analogously: in fact, we consistently observed

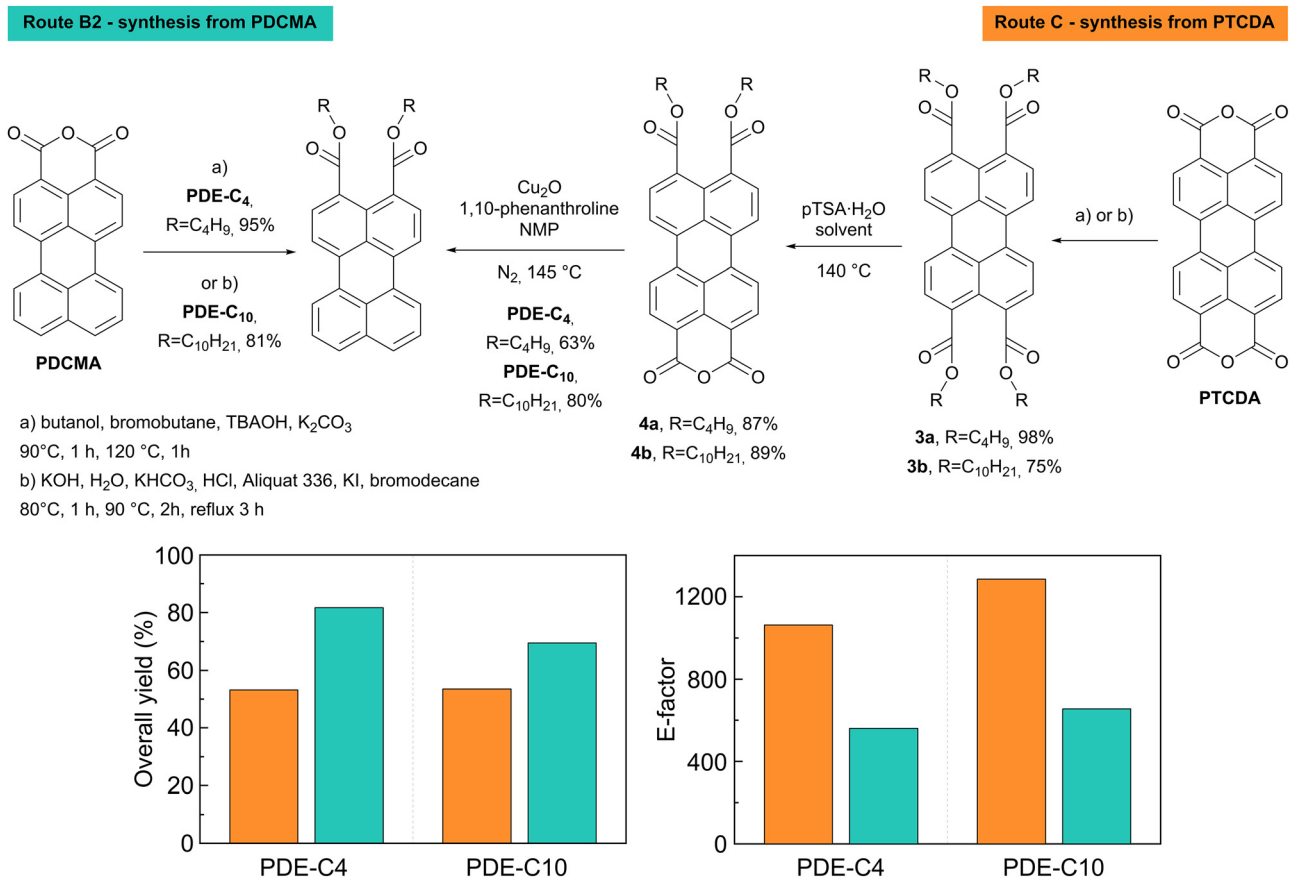

Fig. 2 Synthesis of **PDE-C4** and **PDE-C10** according to route B2 and C, and associated overall yields (starting from the commercially available precursors **PTCDA** and **1** respectively) and *E*-factors for their preparation.

formation of polybromination products while the reagent was still present. Despite thoroughly testing alternative reaction conditions, we were unable to achieve full reagent conversion without the formation of polybromination byproducts (see SI for further details).

Bromination of **PDEs** in the same conditions used for PDIs was ruled out due to the formation of polybromination products, and we resorted to the conditions reported by Xiao and coworkers (Br_2 and K_2CO_3 in $CHCl_3$, derivatives **6a** and **6b**).

Having bromides in our hands, we finally proceeded toward the preparation of 3,3′-biperylenes *via* nickel-catalysed Yamamoto reductive coupling. We tested the reaction using both $NiCl_2$ in the presence of PPh_3, and Ni(dppf)Cl_2 in the presence of dppf as the catalytic system, in both cases preparing the Ni(0) species by *in situ* reduction with zinc dust. The reaction works nicely in all cases, both on PMIs and PDEs, affording the dimers in 61% to 86% yields. The best results were obtained using Ni(dppf)Cl_2/dppf for PDIs, and $NiCl_2$/PPh_3 for PDEs.

We finally tested the possibility to prepare PMI dimers by transamidation reaction from **BPTE-C4**, finding that performing the reaction in imidazole in the presence of $Zn(OAc)_2$ allows to prepare **BPDI-HD** in a satisfactory 73% yield. A little amount of monoimidation product (~9%) was also isolated from the reaction, allowing to record its optical properties (see Fig. S1 in the SI). The reaction also works with the poorly nucleophilic 2,6-diisopropylaniline, even though the double-imidated product is obtained in a more modest 43% yield.

Besides BPTCA derivatives, the optimized preparation of PDEs extends the synthetic playground to all the functionalizations already known for PMIs (*e.g.* Suzuki–Miyaura and Sonogashira couplings, Buchwald–Hartwig amination, *peri* annulation and so on).[20] In this regard, we tested the Buchwald–Hartwig amination of **6b** with dibenzoazepine[21] (Scheme 3), obtaining the target product **7** in 86% yield.

Optical characterization and solubility

The photophysical properties of the synthesized PMIs, PDEs, and their corresponding 3,3′-biperylenes (**BPDIs**, **BPTEs**) were investigated by UV-vis absorption and steady-state photoluminescence spectroscopy in chloroform, complemented by solubility assessment (Table 1 and Fig. 3). Properties for two **PTCDA** derivatives (**PDI-HD** and 3,4,9,10-perylenetetracarboxylic acid tetrabutylester, from now on **PTE-C4**) are also added for comparison.

All derivatives containing a single perylene unit display the characteristic vibronically structured absorption bands of perylene chromophores in the visible region (450–550 nm), with molar extinction coefficients on the order of $4 \times 10^4\ M^{-1}\ cm^{-1}$. The trend in the optical gap reflects both the number and the strength of the electron-withdrawing substituents, following

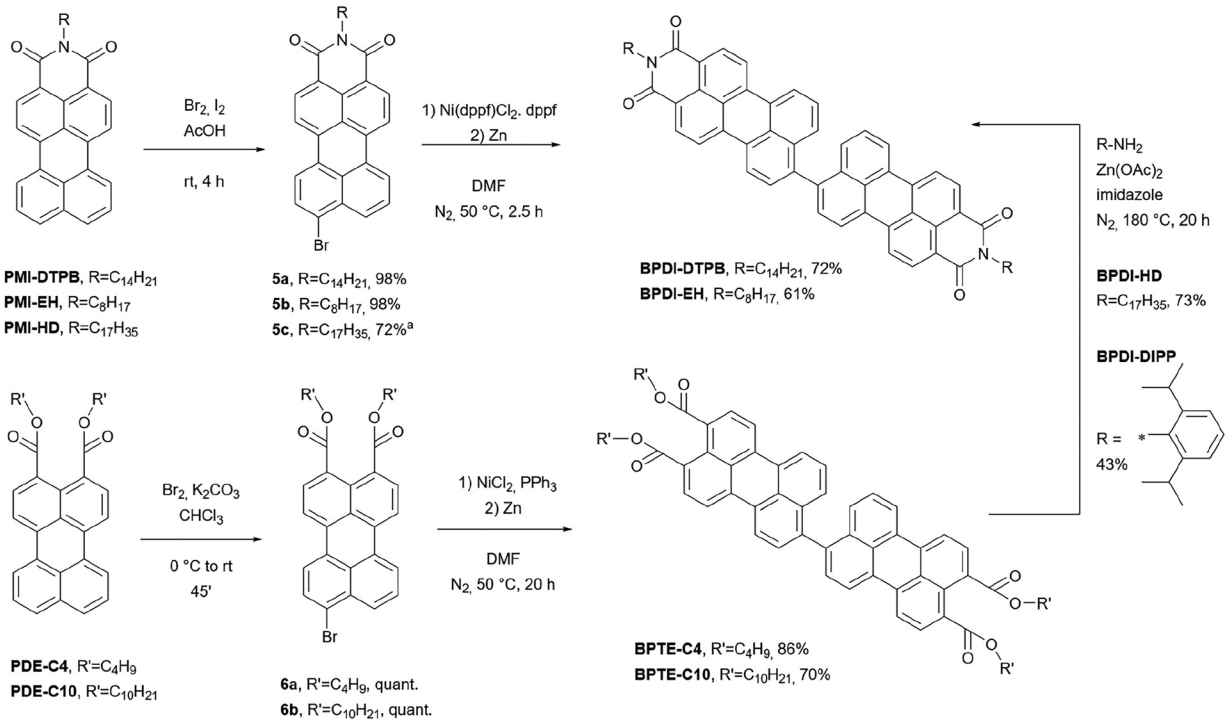

Scheme 2 Synthetic pathway for the preparation of **BPDIs** and **BPDEs** dyads. [a]The product is contaminated by unreacted reagent. An alternative procedure to isolate the pure product is reported in Section S3.3 of the SI.

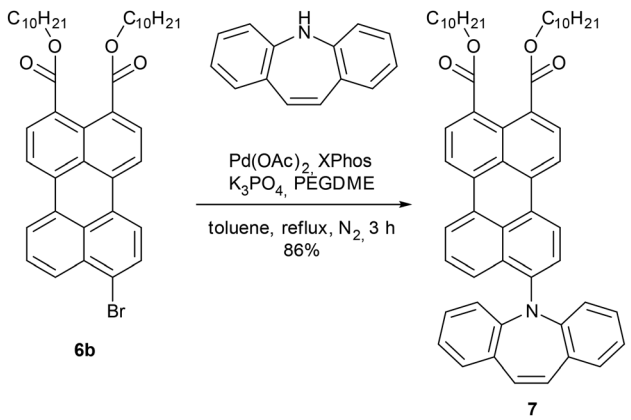

Scheme 3 Buchwald–Hartwig amination of diester **6b** with dibenzoazepine to give the donor–acceptor chromophore **7**.

the sequence (from larger to smaller gap): PDEs > PTEs > PMIs > PDIs. Notably, the nature of the ester *versus* imide substituents has only a limited impact on the optical properties (Fig. 3).

The absorption profiles of the BPTCA derivatives closely resemble those of the corresponding monomers. In contrast, the emission spectra show pronounced differences. While monomeric PMIs exhibit moderately structured emission with Stokes shifts of approximately 150 meV, the corresponding dimeric **BPDIs** display significantly larger values ($\approx$256 meV), which are markedly higher than those typically observed for PDIs ($\approx$27 meV). Relative quantum yields (estimated using **PTE-C4** or **PMI-EH** as the references, see Section S6 of SI for details) lie around 90% for **BPTEs** and 80% for **BPDIs**, consistently with existing literature.[17,22]

As discussed in the literature, BPTCA derivatives can be described as twisted chromophores. In such systems, the ground state is characterized by a non-planar, weakly conjugated structure, while upon photoexcitation the compounds quickly relax into lower energy planarized structures (as also confirmed by DFT calculations).[17] This substantial reorganization of the structure upon excitation results in a bathochromically shifted emission and in larger Stokes shifts.[18,23] The essentially absent solvatochromic response observed for both **BPDI-HD** and **BPTE-C4** further supports this interpretation, indicating that symmetry-breaking charge separation does not dominate the excited state (see Fig. S2 and S3 in the SI, and the comparison of absorption and PL spectra of **PDE-C4** and **PTE-C4** in the selected solvents).

A comparison with representative perylenediimides highlights the advantages of these systems. While PDIs typically exhibit narrow, mirror-image absorption and emission spectra with very small Stokes shifts, **BPDIs** and **BPTEs** combine similarly strong absorption with significantly larger spectral separation. These features are particularly advantageous for applications requiring suppression of self-absorption, such as luminescent solar concentrators and scintillators, where reabsorption losses critically limit performance.

A further advantage of such twisted chromophores emerges when comparing them with conventional donor–acceptor

Table 1 UV-Vis characteristics of the synthesized derivatives (molar extinction coefficient ε, absorption and PL emission maxima, Stokes shift), and their solubility in $CHCl_3$

Compound	ϕ_{rel}[a]	ε (M^{-1} cm^{-1})	λ_{max}^{abs} (nm)	λ_{max}^{PL} (nm)	Stokes shift (meV)	Solubility (μmol mL^{-1})
PDE-C4	0.95 ± 0.1	30 800	461	490	159	320 (144 mg mL^{-1})
BPTE-C4	0.89 ± 0.09	85 000	479	543	305	250 (225 mg mL^{-1})
BPTE-C10	0.88 ± 0.09	86 000	479	542	301	200 (248 mg mL^{-1})
PTE-C4	1[24]	32 410[24]	472	491	101	417 (272 mg mL^{-1})
PMI-HD	1.0 ± 0.1	32 530[14]	482 (505)[c]	537	146	112 (63 mg mL^{-1})
PMI-EH	0.96[25]	32 400	484 (507)[c]	537	137	100 (43 mg mL^{-1})
PMI-DTBP	0.99 (ref. 26)[b]	35 300[14]	489 (512)[c]	535	104	50 (25 mg mL^{-1})
BPDI-HD	0.83 ± 0.08	101 000	526	590	256	150 (168 mg mL^{-1})
BPDI-EH	0.75 ± 0.08	93 000	528	594	261	77 (66 mg mL^{-1})
BPDI-DTBP	0.84 ± 0.08	94 000	528	599	278	39 (40 mg mL^{-1})
PDI-HD	1.0 ± 0.1	77 400	525	531	27	117 (101 mg mL^{-1})

[a] Relative quantum yield (reference: **PTE-C4** for ester derivatives, **PMI-EH** for imide derivatives. λ^{exc} = 420 nm). [b] Quantum yield in toluene. [c] The peak in parentheses is used to calculate the Stokes shift.

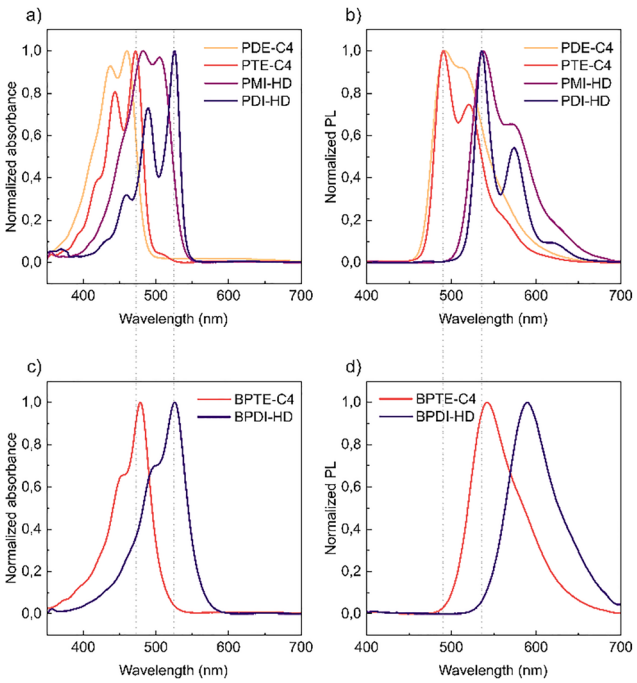

Fig. 3 Normalized UV-vis absorption and PL spectra in $CHCl_3$ of (a) and (b) **PDE-C4**, **PTE-C4**, **PMI-HD** and **PDI-HD**, and (c) and (d) the corresponding dimers **BPTE-C4** and **BPDI-HD**. Vertical lines are guides for the eye.

systems such as compound 7. Owing to its directional charge-transfer character, involving electron density redistribution from the π-rich dibenzoazepine donor to the ester acceptor units, compound 7 exhibits pronounced solvatochromism, as also observed in related imide derivatives (Fig. 4).[18,27] As a result, its emission properties are strongly dependent on the polarity of the surrounding medium, which can be problematic for applications in solid matrices. As widely reported in the luminescent solar concentrator literature, the optical properties of such donor–acceptor systems are highly sensitive to the polarity of the host material, limiting the ability to tune and reproduce device performance.[28,29]

In contrast, BPTCA derivatives display minimal sensitivity to environmental polarity, ensuring more consistent optical behaviour across different media.

In addition to their optical properties, the synthesized derivatives exhibit markedly improved solubility. While PDIs typically suffer from strong π–π stacking and limited solubility in common organic solvents, the reduced symmetry and the presence of sterically demanding substituents in **BPDIs** and **BPTEs** result in significantly enhanced solubility (up to 168 mg mL^{-1} for **BPDI-HD** and 248 mg mL^{-1} for **BPTE-C10** in chloroform).

This feature on one side facilitates purification and solution handling, but also enables processing strategies that are generally inaccessible to conventional PDIs. In particular, both **BPDI-HD** and **BPTE-C4** can be dissolved at functional concentrations in a commercially available, highly viscous photopolymerizable methacrylic resin used for 3D additive manufacturing (further details on the resin are reported in the Experimental section). This represents a significant practical advantage, as the poor solubility and strong aggregation propensity of PDIs typically prevent their homogeneous incorporation into such matrices.

As shown in Fig. 5, the resulting formulation can be directly photopolymerized in a cylindrical mould without phase separation or scattering defects formation, yielding transparent, luminescent solid objects. Crucially, spectroscopic analysis of the polymerized samples reveals a substantial suppression of aggregation within the solid matrix, even at relatively high chromophore loadings. This is reflected in the preservation of the shape of the PL spectra for both **BPDI-HD** and **BPTE-C4** spectra, while a more marked reabsorption is observed for **PDI-HD** and **PTE-C4**.

Such behaviour is highly advantageous for photonic applications, where aggregation-induced quenching and spectral narrowing typically limit performance. To estimate the impact of reabsorption, we analysed the variation of the PL edges with dye concentration in methyl methacrylate (measurements in the resin are not possible due to the luminescence of the photoinitiator, see Fig. S6 of SI). PL edges gradually shifts at lower energy with increasing dyes concentration for all the derivatives

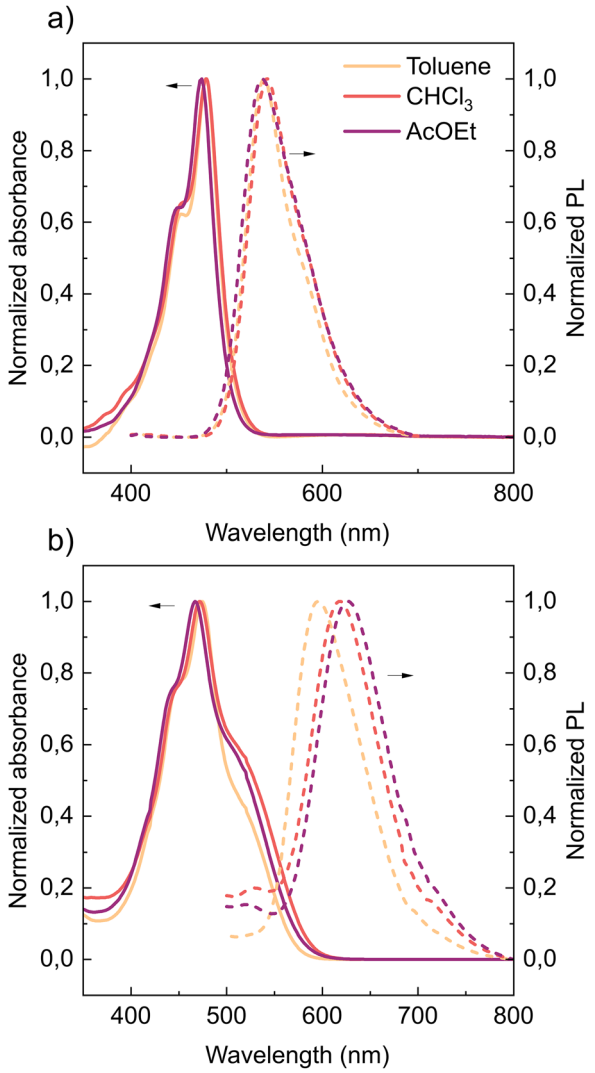

Fig. 4 Normalized absorption and PL spectra of (a) **BPTE-C4** and (b) derivative **7** in different solvents (toluene, $CHCl_3$, AcOEt).

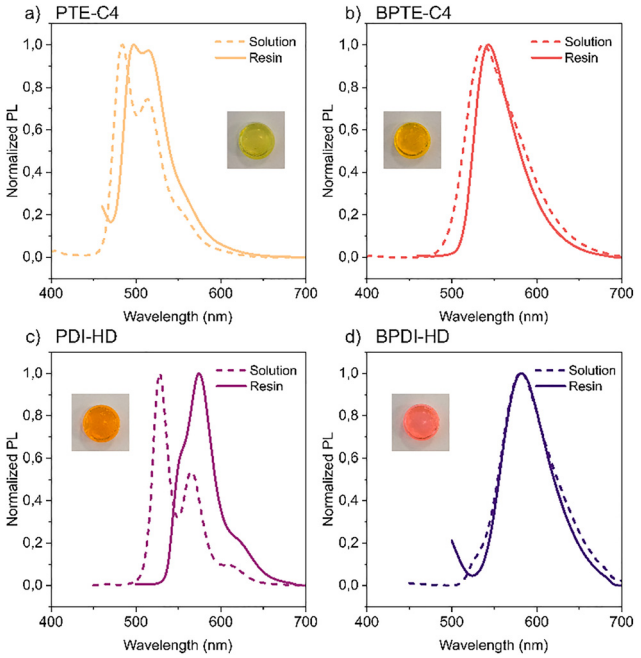

Fig. 5 Normalized PL spectra of (a) **PTE-C4**, (b) **BPTE-C4**, (c) **PDI-HD** and (d) **BPDI-HD** in AcOEt solution ($c = 5 \times 10^{-6}$ M, dashed lines) and in solid sample of photopolymerized resin ($c = 2 \times 10^{-4}$ M, solid lines). A picture of each sample is shown as the inset in the corresponding graphic. The residual PL observed below 500 nm in graphs a and d is due to the photoinitiator present in the resin.

(see SI, Fig. S7–S10 and Table S1), however **BPTE-C4** and **BPDI-HD** retain respectively 75% and 70% of the integrated PL intensity, while the figure drops to 57% and 51% for **PTE-C4** and **PDI-HD** due to their stronger reabsorption.

The ability to maintain emissive efficiency and spectral separation at high dye concentrations directly translates into improved light harvesting and reduced reabsorption losses, making these materials particularly attractive for luminescent solar concentrators and scintillators fabricated *via* scalable 3D printing approaches. The compatibility with commercially available photopolymerizable resins further highlights the potential for direct integration into scalable manufacturing workflows. Overall, these results demonstrate that the synthetic accessibility enabled by **PDCMA** is not merely a preparative advantage, but translates into distinct and functionally relevant photophysical properties, reinforcing the potential of these materials as alternatives to conventional PDIs.

Conclusions

In this work, we demonstrate an optimized synthetic access to a library of 3,3′-biperylene-9,9′,10,10′ tetracarboxylic acid derivatives in the form of both esters (**BPTEs**) and diimides (**BPDIs**) overcoming longstanding synthetic limitations associated with the preparation of this high performing systems. In doing so we took advantage of our recently published sustainable and scalable synthesis of 3,4-perylenedicarboxylic monoanhydride (**PDCMA**) as a practical starting point. By systematically comparing alternative synthetic routes, we show that **PDCMA**-based strategies offer clear advantages in terms of yield, operational simplicity, and environmental impact, enabling access to these chromophores under significantly improved sustainability metrics.

The resulting materials retain the high absorption coefficients typical of perylene based chromophores while exhibiting markedly enhanced photophysical behaviour. In particular, the reduced environmental sensitivity due to nearly absent solvatochromism is a key advantage for applications in solid-state media.

A central outcome of this work is the demonstration that the improved solubility and reduced aggregation propensity of **BPDIs** and **BPTEs** translate directly into enhanced processability. In particular, these chromophores can be homogeneously incorporated into commercially available photopolymerizable resins and processed into transparent, luminescent objects. The suppression of aggregation within the polymer matrix grants the preservation of large Stokes shifts and limited reabsorption even at relatively high dye loadings, addressing a major limitation of conventional perylene-based systems.

Overall, this work highlights how improved synthetic accessibility can unlock not only new molecular architectures but also new processing strategies and application opportunities. The combination of sustainable synthesis, favourable photophysics, and compatibility with advanced manufacturing approaches positions BPTCA derivatives as promising candidates for wavelength-shifting technologies, including luminescent solar concentrators and scintillators.

Experimental

Materials and methods

Commercial grade reagents and solvents were used without further purification. Formlab photopolymer resin clear (FLGPCL04) was used for solid samples preparation.

Reactions are monitored by TLC on 0.20 mm thick Polygram Sil G/UV254 silica gels. Solution optical absorption and emission spectroscopy were performed in a 1 cm optical path quartz cuvette using a PerkinElmer Lambda 1050+ spectrophotometer and a Jasco FP-6200 spectrofluorometer respectively.

NMR spectra were recorded with a Bruker NMR Avance 400 NEO instrument operating at 400 MHz ^{1}H and 101 MHz ^{13}C. Resonance frequencies refer to tetramethylsilane (TMS).

Details on synthetic procedures

PMI-DTBP (route B1). In a 250 mL roundbottom flask, **PDCMA** (1.625 g, 5.04 mmol), $Zn(OAc)_2$ (550 mg, 2.51 mmol), 3,5-di-*tert*-butylaniline (1.245 g, 6.06 mmol) and imidazole (31.06 g) are put under nitrogen atmosphere, then the reaction is heated to 140 °C. The mixture is stirred at 140 °C for 5 h and the reaction is monitored *via* TLC using DCM as the eluent. The reaction is cooled down to ~80 °C, then HCl 2 M solution (250 mL) is added and the mixture it is heated to reflux for 1 h. A precipitate forms, which is filtered and dried. The crude is purified by filtration on a silica pad using a solution of heptane/DCM 1 : 4 (450 mL of eluent are used). 2.01 g of pure product are obtained as a bright red powder (3.94 mmol, 78% yield). ^{1}H NMR (400 MHz, CDCl3) δ 8.63 (d, 2H, J = 8 Hz), 8.43 (t, 4H, J = 6.4 Hz), 7.90 (d, 2H, J = 8 Hz), 7.62 (m, 3H), 7.46 (dd, J = 8.4, 2.0 Hz, 1H), 7.04 (s, 1H), 1.34 ppm (s, 9H), 1.30 ppm (s, 9H).[14]

PMI-EE (route B1). In a 100 mL roundbottom flask, **PDCMA** (322 mg, 1.00 mmol) and imidazole (2 g) are put under nitrogen atmosphere, then the reaction is heated to 140 °C and the amine (143 mg, 1.10 mmol) is finally added. The mixture is stirred at 140 °C for 3 h and the reaction is monitored *via* TLC (heptane/DCM 1 : 3). The reaction is cooled down to ~80 °C, then HCl 2 M solution (20 mL) is added and the mixture it is heated to reflux for 1 h. A precipitate forms, which is filtered and dried. The crude is purified by filtration on a silica pad using a solution of heptane/DCM 1 : 1 (80 mL of eluent are used). 423 mg of pure product are obtained as a bright red powder (0.976 mmol, 98% yield). ^{1}H NMR (400 MHz, $CDCl_3$) δ 8.58 (d, 2H, d, J = 8 Hz), 8.41 (4H, m), 7.90 (d, 2H, J = 9 Hz), 7,62 (t, 2H, J = 8 Hz), 4.14 (2H, m), 1.97 (1H, m), 1.37 (8H, m), 0.97 (t, 3H, J = 14 Hz), 0.91 (t, 3H, J = 14 Hz).[30]

PMI-HD (route B1). In a 100 mL roundbottom flask, **PDCMA** (1.50 g, 4.66 mmol) and imidazole (9.3 g) are put under nitrogen atmosphere, then the reaction is heated to 140 °C and the amine (1.30 g, 5.09 mmol) is finally added. The mixture is stirred at 140 °C for 3 h and the reaction is monitored *via* TLC (heptane/DCM 1 : 3). The reaction is cooled down to ~80 °C, then HCl 2 M solution (200 mL) is added and the mixture it is heated to reflux for 1 h. A precipitate forms, which is filtered and dried. The crude is purified by filtration on a silica pad using a solution of heptane/DCM 1 : 1 (250 mL of eluent are used). 1.75 g of pure product are obtained as a bright red powder (3.29 mmol, 71% yield). ^{1}H NMR (400 MHz, $CDCl_3$) δ 8.54 (2H, m), 8.39 (4H, t, J = 9 Hz), 7.86 (2H, d, J = 8 Hz), 7.61 (t, 2H, J = 8 Hz), 5.20 (1H, s), 2.24 (2H m), 1.86 (2H, m), 1.25 (m, 25H), 0.84 ppm (t, 6H, J = 6.5 Hz).[14]

PDE-C4 (route B2). PDCMA (1.50 g, 4.66 mmol) is introduced into a 100 mL two-necked round bottom flask. The system is placed in nitrogen atmosphere. The solid is dispersed in 10 mL of 1-butanol and TBAOH 40 wt% (4.0 mL, 6.17 mmol), and the dispersion is heated at 50 °C for 20 min. Finely milled K_2CO_3 (1.00 g, 4. 56 mmol) and 1-bromobutane (17 mL, 21.7 g, 106 mmol) are then added and the reaction mixture is heated to 120 °C for 6 h. The reaction mixture is diluted with 60 mL of toluene and filtered on a Celite pad, then washed with aqueous K_2CO_3 1 wt% (3 × 50 mL) and then water (3 × 50 mL). The organic phase is dried on anhydrous $MgSO_4$ and the solvents removed by vacuum distillation. The crude is finally purified by filtration on a silica pad (heptane/DCM 1 : 4 as eluent, 250 mL). A bright orange solid is obtained (2.01 g, 4.44 mmol, 95% yield). ^{1}H NMR (400 MHz, $CDCl_3$) δ 8.12 (dd, J = 12.4, 7.7 Hz, 4H), 7.95 (d, J = 7.9 Hz, 2H), 7.70 (d, J = 7.9 Hz, 2H), 7.44 (t, J = 7.8 Hz, 2H), 4.33 (t, J = 6.9 Hz, 4H), 1.83 – 1.74 (m, 4H), 1.50 (dq, J = 14.7, 7.4 Hz, 4H), 1.00 (t, J = 7.4 Hz, 6H).[12]

PDE-C10 (route B2). In a two-necked 500 mL round bottom flask, **PDCMA** (1.00 g, 3.10 mmol) and pulverized KOH 85 wt% (0.82 g, 12.4 mmol) are introduced and dispersed in 45 mL of deionized water, the mixture is heated at 80 °C for 2 h. After cooling to rt, KI (0.417 g, 2.51 mmol), TOAB (1.37 g, 2.51 mmol) and 1-bromodecane (2.06 g, 9.3 mmol, 1.93 mL) are added. The mixture is heated at reflux temperature overnight. The reaction is monitored by TLC, using a solution of DCM/*n*-heptane 8 : 2 as eluent. The reaction mixture is then cooled down at rt and extracted with 3 × 200 mL of DCM. The organic phase is washed with brine and dried on anhydrous $MgSO_4$, the solvent is removed under reduced pressure and a brown solid is obtained. The crude solid is purified by flash chromatography using a solution of DCM/*n*-heptane 8 : 2 as eluent. An orange solid is obtained (1.70 g, 88%). ^{1}H NMR (400 MHz, $CDCl_3$) δ 8.31 (d, J = 7.2 Hz, 2H), 8.26 (d, J = 8.0 Hz, 2H), 8.03 (d, J = 7.9 Hz, 2H), 7.80 (d, J = 7.9 Hz, 2H), 7.56 (t, J = 7.8 Hz, 2H), 4.30 (t, J = 6.9 Hz, 4H), 1.82 – 1.73 (m, 4H), 1.47 – 1.21 (m, 28H), 0.87 (t, J = 6.9 Hz, 6H). ^{13}CNMR (101 MHz, $CDCl_3$) δ 168.97, 134.50, 134.11, 130.42, 129.77, 129.60, 129.19, 129.07, 127.73, 126.70, 122.14, 119.41, 65.49, 32.02, 29.69, 29.49, 29.44, 28.77, 26.18, 22.80, 14.22.[15]

BPDI-DTBP. In a 100 mL roundbottom flask Ni(dppf)Cl_2 (684 mg, 1.00 mmol) and dppf (1.108 g, 2.00 mmol) are put under

nitrogen atmosphere and 10 mL of anhydrous DMF are added. The solution is stirred and heated at 50 °C for 30 minutes, then zinc dust (130 mg, 2.00 mmol) is added. The mixture is left for 2 h at 50 °C. In a second 100 mL roundbottom flask, **5a** (589 mg, 1.00 mmol) is put under nitrogen atmosphere and 10 mL of anhydrous DMF are added. The dispersion is stirred for 2 h, then the mixture obtained in the first flask is added dropwise into the second flask. The reaction is monitored by TLC (toluene/DCM 2 : 1). After 4 h the reaction is quenched pouring the mixture into a 50 mL solution of HCl 2 M under stirring for 1 h. A precipitate forms, which is filtered and washed with water. A red/purple crude is obtained, which is purified by gradient elution column chromatography (toluene/DCM 1 : 1 to toluene/DCM 1 : 2). The product is isolated as a dark red powder (400 mg, 78.7% yield). ^{1}H NMR (400 MHz, $CDCl_3$) δ 8.74–8.69 (m, 4H), 8.66–8.63 (m, 2H), 8.59–8.51 (m, 6H), 7.77–7.74 (m, 2H), 7.62–7.58 (m, 4H), 7.56–7.51 (m, 2H), 7.47 (dd, J = 8.6, 2.2 Hz, 2H), 7.05–7.04 (m, 2H).[8]

BPDI-EE. In a 50 mL roundbottom flask Ni(dppf)Cl_2 (680 mg, 0.995 mmol) and dppf (1.103 g, 1.99 mmol) are put under nitrogen atmosphere and 15 mL of anhydrous DMF are added. The solution is stirred and heated at 50 °C for 30 minutes, then zinc dust (130 mg, 2.00 mmol) is added. The mixture is left for 2 h at 50 °C. In a second 100 mL roundbottom flask, **5b** (510 mg, 0.995 mmol) is put under nitrogen atmosphere and 7 mL of anhydrous DMF are added. The dispersion is stirred for 2 h, then the mixture obtained in the first flask is added dropwise into the second flask. The reaction is monitored by TLC (toluene/DCM 2 : 1). After 3 h the reaction is quenched pouring the mixture into a 50 mL solution of HCl 2 M under stirring for 1 h. A precipitate forms, which is filtered and washed with water. A red/purple crude is obtained, which is purified by gradient elution column chromatography (toluene to toluene/AcOEt 9 : 1). The product is isolated as a dark red powder (264 mg, 61.3% yield). Mp 328 °C. ^{1}H NMR (400 MHz, $CDCl_3$) δ 8.75 (6 H, t, J = 8 Hz), 8.63 (6 H, m), 7.82 (2H, d, J = 8 Hz), 7.69 (2H, d, J = 8 Hz), 7.60 (2 H, t, J = 8 Hz), 4.14 (4H, m), 1.97 (2H, m), 1.37 (16H, m), 0.97 (t, 6H, J = 14 Hz), 0.91 (t, 6H, J = 14 Hz) ppm. ^{13}C NMR (101 MHz, $CDCl_3$) δ 166.35, 162.56, 162.12, 161.69, 161.26, 141.46, 139.16, 138.93, 133.52, 133.46, 130.43, 129.85, 129.48, 129.01, 128.96, 127.92, 127.70, 126.54, 125.36, 124.57, 120.96, 120.82, 119.28, 119.20, 118.33, 115.50, 112.68, 109.85, 77.04, 45.36, 37.92, 30.59, 28.47, 23.84, 22.88, 13.62, 10.22 ppm. Anal. Calcd for $C_{60}H_{52}N_2O_4$: C, 83.31; H, 6.06; N, 3.24. Found: C, 83.20; H, 6.15; N, 3.13.

BPDI-HD. In a 100 mL roundbottom flask **BPTE-C4** (200 mg, 0.221 mmol), heptadecan-9-amine (566 mg, 2.2 mmol), $Zn(OAc)_2{\cdot}H_2O$ (80 mg, 0.44 mmol) and imidazole (600 mg) are put under nitrogen atmosphere. The mixture is heated at 140 °C overnight (18 hours). The reaction is monitored by TLC (heptane/DCM 3 : 1). The reaction is cooled down to 80 °C, then 50 mL of HCl 2 M are added into the flask, and the mixture is refluxed for 1 h. A waxy precipitate forms, which is filtered, triturated with methanol, filtered again and dried. A purple crude is obtained, which is purified by filtration over a silica pad using toluene as eluent. The product is isolated as a dark red waxy powder (180 mg, 73% yield). Further elution allowed to isolate a small amount of a different product, which was later identified as the monoimidation product (identified as derivative **8**, see SI, Section S3.4). Mp 246 °C. ^{1}H NMR (400 MHz, $CDCl_3$) δ 8.59 (6 H, m), 8.48 (2H, d, J = 8 Hz), 8.42 (4H, m), 7.72 (2H, d, J = 8Hz), 7.55 (2H, d, J = 8 Hz), 7.49 (2 H, t, J = 8 Hz), 5.20 (2H, s), 2.24 (4H, m), 1.86 (4H, m), 1.25 (m, 50 H), 0.84 (t, 12H, J = 6,5Hz) ppm. ^{13}C NMR (101 MHz, $CDCl_3$) δ 140.35, 133.65, 129.94, 129.63, 129.56, 129.15, 128.26, 127.30, 126.59, 123.73, 123.09, 120.46, 120.33, 54.47, 32.43, 31.81, 29.59, 29.51, 29.24, 27.01, 22.61, 14.05 ppm. Anal. Calcd for $C_{78}H_{88}N_2O_4$: C, 83.83; H, 7.94; N, 2.51. Found: C, 83.70; H, 8.10; N, 2.45.

BPDI-DIPP. In a 50 mL roundbottom flask **BPTE-C4** (200 mg, 0.221 mmol), 2,6-diisopropylaniline (392 mg, 2.21 mmol), $Zn(OAc)_2$ (60.2 mg, 0.442 mmol) and imidazole (601 mg) are put under nitrogen atmosphere. The mixture is heated at 180 °C overnight (18 hours). The reaction is monitored by TLC (toluene/DCM 1 : 2). The reaction is cooled down to 80 °C, then 50 mL of HCl 2 M are added into the flask, and the mixture is refluxed for 1 h. A waxy precipitate forms, which is filtered, triturated with ethanol, filtered again and dried. A purple crude is obtained, which is purified by gradient elution column chromatography (toluene/DCM 1 : 1 to toluene/DCM 1 : 2). The product is isolated as a dark red powder (92 mg, 43% yield). Mp > 340 °C. ^{1}H NMR (400 MHz, $CDCl_3$) δ 8.73 (t, J = 8.0 Hz, 4H), 8.67 (d, J = 8.0 Hz, 2H), 8.60 (d, J = 8.2 Hz, 2H), 8.55 (dd, J = 8.0, 2.0 Hz, 4H), 7.76 (d, J = 7.7 Hz, 2H), 7.64 (d, J = 8.4 Hz, 2H), 7.59 – 7.47 (m, 4H), 7.36 (d, J = 7.8 Hz, 4H), 2.84–2.76 (m, 4H), 1.21 (dd, J = 6.7, 3.9 Hz, 24H) ppm. ^{13}C NMR (100 MHz, CDCl3) δ 163.96, 145.72, 145.68, 140.53, 137.44, 137.23, 133.69, 132.14, 130.97, 130.56, 129.63, 129.57, 129.49, 129.38, 129.27, 128.31, 127.47, 126.99, 124.09, 124.05, 123.41, 121.31, 121.26, 120.60, 120.46, 29.16, 24.04 ppm. Anal. Calcd for $C_{72}H_{60}N_2O_4$: C, 85.01; H, 5.95; N, 2.75. Found: C, 84.80; H, 6.12; N, 2.70.

BPTE-C4. In a 250 mL two necked roundbottom flask, $NiCl_2$ (279 mg, 2.15 mmol) and PPh_3 (2.258 g, 8.608 mmol) are weighted and put under nitrogen atmosphere. Anhydrous DMF (32 mL) is added, and the reaction is heated up to 50 °C. After 10 minutes, Zn dust (281 mg, 4.30 mmol) is added. Over time, the reaction changes color from light blue to green to brown/red. After 2 hours, **6a** (1.144 g, 2.152 mmol) is added, and the reaction is kept at 50 °C for 1.5 hours. Upon completion, the mixture is cooled down to room temperature, and filtered. The filtrate is poured into 150 mL of EtOH, the precipitate is filtered. The obtained solid is dissolved in THF and filtered on a Celite pad using THF as eluent, the solvent is removed under reduced pressure. The solid is finally hot filtered from 50 mL of EtOH, and dried until weight stabilization. Orange powder, 830 mg (0.919 mmol, 85.4% yield). Mp 195 °C. ^{1}H NMR (400 MHz, $CDCl_3$) δ 8.38 (2H, d, J = 4 Hz), 8.27 (6H, m), 8. 03 (4H, t, J = 8Hz), 7.58 (2H, d, J = 4 Hz), 7.46 (2H, d, J = 8 Hz), 7.37 (2H, t, J = 8 Hz), 4.43 (8H, t, J = 7 Hz), 1.81 (8H, m), 1.53 (8H, m), 1.01 (12H, t, J = 7 Hz) ppm. ^{13}C NMR (101 MHz, $CDCl_3$) δ 169.90, 140.01, 135.34, 135.16, 134.27, 131.29, 130.96, 130.78, 130.34, 130.31, 130.10, 130.05, 129.62, 128.78, 128.58, 127.80, 123.16, 122.59, 120.53, 120.36, 65.59, 31.42, 19.40, 13.90

ppm. Anal. Calcd for $C_{60}H_{54}O_8$: C, 79.80; H, 6.03. Found: C, 79.67; H, 6.08.

BPTE-C10. In a 100 mL two necked roundbottom flask, $NiCl_2$ (185.2 mg, 1.429 mmol) and PPh_3 (1.500 g, 5.716 mmol) are weighted and put under nitrogen atmosphere. Anhydrous DMF (34 mL) is added, and the reaction is heated up at 50 °C. After 20 minutes, Zn dust (186.9 mg, 2.858 mmol) is added. In 30 minutes, the reaction changes color from light blue to green to brown/red. After 1 hour, **6b** (1.000 g, 1.429 mmol) is added, and the reaction is kept at 50 °C overnight (20 hours). The reaction is monitored by TLC (heptane/DCM 2 : 8). Upon completion, the mixture is cooled down to room temperature and poured into 150 mL of EtOH and stirred for 10 minutes. An orange precipitate forms, which is filtered and further washed with EtOH. The solid is dissolved in $CHCl_3$ and filtered on a Celite pad using $CHCl_3$ as eluent, then the solvent is removed under reduced pressure. The solid is triturated with 20 mL of EtOH, filtered and dried until weight stabilization. Orange powder, 621 mg (0.501 mmol, 70.1% yield). Mp 203 °C. ^{1}H NMR (400 MHz, $CDCl_3$) δ 8.43 (2H, d, J = 8 Hz), 8.32 (6 H, m), 8.07 (4H, t, J = 8 Hz), 7.61 (2H, d, 8 Hz), 7,47 (2H, d. J = 8 Hz), 7.41 (2H, t, J = 8Hz), 4.28 (8 H, t, J = 7 Hz), 1.78 (8 H, quint, J = 6,5 Hz), 1.30 (56 H, m), 0.88 (12H, t, J = 7Hz) ppm. ^{13}C NMR (101 MHz, $CDCl_3$) δ 169.89, 140.06, 135.39, 135.22, 134.33, 131.34, 131.03, 130.85, 130.39, 130.36, 130.13, 130.09, 130.36, 130.14, 130.09, 129.66, 128.82, 128.64, 127.84, 123.17, 122.61, 120.56, 120.40, 69.92, 32.10, 29.74, 29.54, 29.50, 28.79, 26.21, 22.82, 14.20 ppm. Anal. Calcd for $C_{84}H_{102}O_8$: C, 81.38; H, 8.29. Found: C, 81.21; H, 8.37.

Details on preparation of photopolymerized resin samples

Photopolymerized resin disks containing **BPTE-C4**, **BPDI-HD** and **PDI-HD** were prepared according to the following procedure.

A stock solution of each derivative was prepared by dissolving the dye powder in 300–400 μL of chloroform and then diluting this solution with 1 mL of resin. The vials containing the solutions were left open and the solution were stirred in the dark for at least 2 hours, to let residual chloroform evaporate and reach a nominal dye concentration of $\sim 2 \times 10^{-3}$ M. 100 μL of these solutions were then diluted with resin to reach a dye concentration of $\sim 2 \times 10^{-4}$ M. 400 μL of the as obtained dyes solutions were then introduced in transparent 4 mL vials and put under blue light irradiation (λ = 460 nm) at rt for 24 hours to give solid polymerized samples.

Due to poorer solubility of **PTE-C4** in the resin, it was not possible to obtain a 10^{-3} M solution for this derivative and a 1×10^{-4} M solution was directly prepared instead and used for the photopolymerization procedure. Fluorescence spectra of the polymerized samples were recorded under excitation with 400 nm light.

Author contributions

Conceptualization: M. S., L. B., S. M. Investigation: L. M., M. S., A. Z., F. P., S. M. Data curation: L. M., S. M. Supervision: M. S., L. B., S. M. Writing – original draft: L. B., S. M. Writing – review & editing: M. S., F. P. Funding acquisition: L. B.

Conflicts of interest

There are no conflicts to declare.

Data availability

The data supporting this article have been included as part of the supplementary information (SI). Supplementary information: additional figures and tables; materials and methods for the preparation of all products and intermediates; details on the calculations of E-factor according to both literature data and the procedure described in this paper; procedure for the estimation of quantum yields; copies of ^{1}H and ^{13}C NMR spectra. See DOI: https://doi.org/10.1039/d6tc01479h.

Acknowledgements

This work has been funded within the framework of the Regional Programme of the European Regional Development Fund 2021–2027 of Regione Lombardia (PR FESR 2021-2027, Action 1.1.3, in compliance with European Regulation No. 1060/2021), following the public call ''Collabora&Innova''. Project ''CO_2: from a global problem to a tool to implement circularity – CO-Tool'' (Project ID 6144755).

References

1 M. Sun, K. Müllen and M. Yin, *Chem. Soc. Rev.*, 2016, **45**, 1513–1528.
2 O. Krupka and P. Hudhomme, *Int. J. Mol. Sci.*, 2023, **24**, 6308.
3 A. A. Mohapatra, M. Pranav, S. Yadav, C. Gangadharappa, J. Wu, C. Labanti, J. Wolansky, J. Benduhn, J.-S. Kim, J. Durrant and S. Patil, *ACS Appl. Mater. Interfaces*, 2023, **15**, 25224–25231.
4 M. J. Alonso-Navarro, F. Suárez-Blas, J. I. Martínez, M. M. Ramos and J. L. Segura, *Org. Lett.*, 2025, **27**, 9613–9618.
5 W. Zhou, G. Liu, B. Yang, Q. Ji, W. Xiang, H. He, Z. Xu, C. Qi, S. Li, S. Yang and C. Xu, *Sci. Total Environ.*, 2021, **780**, 146483.
6 R. Roy, A. Khan, O. Chatterjee, S. Bhunia and A. L. Koner, *Org. Mater.*, 2021, **3**, 417–454.
7 R. Roy, A. Khan, T. Dutta and A. L. Koner, *J. Mater. Chem. B*, 2022, **10**, 5352–5363.
8 M. Gandini, I. Villa, M. Beretta, C. Gotti, M. Imran, F. Carulli, E. Fantuzzi, M. Sassi, M. Zaffalon, C. Brofferio, L. Manna, L. Beverina, A. Vedda, M. Fasoli, L. Gironi and S. Brovelli, *Nat. Nanotechnol.*, 2020, **15**, 462–468.
9 H. Langhals and A. Hofer, *J. Org. Chem.*, 2012, **77**, 9585–9592.
10 H. Langhals and F. Sussmeier, *J. Prakt. Chem.*, 1999, **341**, 309–311.

11 H. Langhals and A. Walter, *J. Phys. Chem. A*, 2020, **124**, 1554–1560.
12 A. Zucchi, S. Mattiello, M. Sassi and L. Beverina, *ACS Sustainable Chem. Eng.*, 2024, **12**, 8533–8540.
13 H. Langhals, P. Von Unold and M. Speckbacher, *Liebigs Ann./Recl.*, 1997, **1997**, 467–468.
14 L. Feiler, H. Langhals and K. Polborn, *Liebigs Ann.*, 1995, **1995**, 1229–1244.
15 L. Chen, K. Zhang, L. Zhu and Y. Xiao, *Ind. Eng. Chem. Res.*, 2015, **54**, 12699–12703.
16 L. Đorđević, H. Sai, Y. Yang, N. A. Sather, L. C. Palmer and S. I. Stupp, *Angew. Chem., Int. Ed.*, 2023, **62**, e202214997.
17 H. Langhals and A. Hofer, *J. Org. Chem.*, 2012, **77**, 9585–9592.
18 H. Langhals, R. Greiner, T. Schlücker and A. C. Jakowetz, *J. Org. Chem.*, 2019, **84**, 5425–5430.
19 R. Arthur Sheldon, *Green Chem.*, 2023, **25**, 1704–1728.
20 R. Roy, A. Khan, O. Chatterjee, S. Bhunia and A. L. Koner, *Org. Mater.*, 2021, **3**, 417–454.
21 E. Ghiglietti, S. Podapangi, S. Mecca, L. Mezzomo, R. Ruffo, M. Sassi, S. Mattiello, T. M. Brown and L. Beverina, *Energy Adv.*, 2022, **1**, 398–401.
22 J. Cremer and P. Bäuerle, *Eur. J. Org. Chem.*, 2005, 3715–3723.
23 R. Turrisi, A. Sanguineti, M. Sassi, B. Savoie, A. Takai, G. E. Patriarca, M. M. Salamone, R. Ruffo, G. Vaccaro, F. Meinardi, T. J. Marks, A. Facchetti and L. Beverina, *J. Mater. Chem. A*, 2015, **3**, 8045–8054.
24 E. Aydin, B. Nisanci, M. Acar, A. Dastan and Ö. A. Bozdemir, *New J. Chem.*, 2014, **39**, 548–554.
25 R. J. Lindquist, K. M. Lefler, K. E. Brown, S. M. Dyar, E. A. Margulies, R. M. Young and M. R. Wasielewski, *J. Am. Chem. Soc.*, 2014, **136**, 14912–14923.
26 S. I. Yang, R. K. Lammi, S. Prathapan, M. A. Miller, J. Seth, J. R. Diers, D. F. Bocian, J. S. Lindsey and D. Holten, *J. Mater. Chem.*, 2001, **11**, 2420–2430.
27 A. Sanguineti, M. Sassi, R. Turrisi, R. Ruffo, G. Vaccaro, F. Meinardi and L. Beverina, *Chem. Commun.*, 2013, **49**, 1618–1620.
28 F. Meinardi, F. Bruni and S. Brovelli, *Nat. Rev. Mater.*, 2017, **2**, 17072.
29 G. Griffini, *Front. Mater.*, 2019, **6**, 1–8.
30 M. Sekita, Á. J. Jiménez, M. L. Marcos, E. Caballero, M. S. Rodríguez-Morgade, D. M. Guldi and T. Torres, *Chem. – Eur. J.*, 2015, **21**, 19028–19040.